Article
DOI: 10.1002/bkcs.12136 S.-R. Lee and Y. Kim BULLETIN OF THE KOREAN CHEMICAL SOCIETY

X-ray Powder Diffraction Study of Molybdenum Oxides Formed From the Thermal Reactions of MoS_2, MoS_2/LiF, and MoS_2/Ag in Air

So-Ram Lee and Youhyuk Kim*

*Department of Chemistry, College of Natural Sciences, Dankook University, Cheonan, Chungnam, 330-714, Korea. *E-mail: hyukim@dankook.ac.kr*
Received August 31, 2020, Accepted October 16, 2020

MoS_2 can generate useful molybdenum oxides by thermally reacting with LiF or Ag nanoparticles (NPs). MoS_2 easily loses sulfide and reacts with oxygen gas upon heating in air to give orthorhombic molybdenum trioxide, α-MoO_3. Morphological changes of α-MoO_3 from 500 to 900°C were investigated using X-ray powder diffraction and scanning electron microscope. The strong diffraction peaks of the (020), (040), and (060) planes at 800°C revealed highly anisotropic growth of the oxides with a layered crystal structure. In the presence of LiF, MoS_2 reacts with oxygen gas to generate Li_2MoO_4 and MoO_2, depending on the LiF concentration. In the presence of Ag NPs, the thermal reactions of MoS_2 at 800 and 900°C give silver molybdates $Ag_2Mo_2O_7$ and Ag_2MoO_4, respectively. These results demonstrate that MoS_2 is an important precursor for generating useful molybdenum oxides on the surface of inert substrates without requiring sophisticated, expensive equipment.

Keywords: X-ray powder diffraction, MoS_2, Molybdenum oxides, Thermal reaction

Introduction

Molybdenum, molybdenum sulfides, and molybdenum oxides are involved in many useful processes, including as alloying elements in steel to increase hardness, as catalysts for selectively oxidizing olefins,[1] as anodes for X-ray tubes, or as nanometer layers for optical devices used in extreme ultraviolet (EUV) lithography.[2] In particular, molybdenum sulfides and molybdenum oxides have been extensively studied because of their potential use in technological applications as superconductors, catalysts, panel displays, gas sensors, smart windows, and electrochromic devices.[3–9]

Molybdenum oxides belong to a group of inorganic materials with interesting properties that exhibit several different complex structures formed from two-dimensional or three-dimensional frameworks of MoO_6 octahedra and MoO_4 tetrahedra. For example, molybdenum trioxide (α-MoO_3) is a layered material with a distorted perovskite lattice (Figure 1). Its thermodynamically stable phase is orthorhombic, where highly asymmetrical MoO_6 octahedra are interconnected with their edges along the [001] direction and interlinked with their corners along [100], resulting in double-layer sheets (Figure 1). Alternatively, the stacking of these double-layered structures along [010] would form α-MoO_3 with its layered sheets predominantly bound by van der Waals interactions.[10] The MoO_6 octahedra are considerably distorted around the central metal with Mo—O bond distances ranging from 1.67 to 2.33 Å (Figure 1). On the other hand, molybdenum dioxide (MoO_2) has a rutile-type structure consisting of MoO_6 octahedron linkages and tunnels that are located inside the framework structure.[11]

Recent research has focused on developing innovative methods for synthesizing molybdenum oxides to give new, advanced materials with interesting properties and structural features. Wang et al.[12] prepared ultralarge α-MoO_3 nanobelts with an average length of 200–300 μm and a uniform width of approximately 0.6–1.5 μm by a facile hydrothermal method using molybdenyl acetylacetonate as the precursor. When considering their lithium storage properties, these nanobelts exhibit much better electrochemical performance than that of conventional nanobelts. MoO_2 is typically prepared by reacting MoO_3 with hydrogen gas at a high temperature to give large particle sizes. This shows the negative effects in developing new electrode materials for lithium storage, such as significant volume changes. To achieve optimal electrochemical properties of electrode materials during lithiation and delithiation, an ion diffusion pathway with a large surface area and short length is required.[13–17] Therefore, new preparation methods for preparation of α-MoO_3 and lithiated MoO_3 should be developed by reacting with lamellar and reactive precursor, such as MoS_2. In this work, we tried to synthesize α-MoO_3 by the thermal reaction of MoS_2 in air. To obtain lithiated MoO_3, the thermal reaction of MoS_2 with LiF in air was also performed. In addition to molybdenum oxides, their composites with other materials (*e.g.*, Ag and carbon nanotubes [CNTs]) are also expected to enhance or alter the properties of other metals through surface modification.[18–21] In particular, silver molybdates, such as Ag_2MoO_4 and $Ag_2Mo_2O_7$, have been used in several applications including ion-conducting glasses, high-temperature lubrication, and gas sensor due to its unique properties such as high electrical

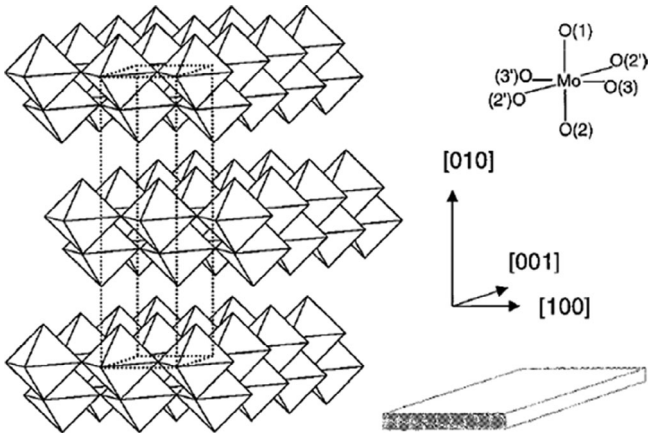

Figure 1. Structure of α-MoO_3 and orientation of crystallographic planes; Mo—O(1) = 1.67 Å, Mo—O(2) = 2.33 Å, Mo—O(2′) = 1.95 Å, Mo—O(3) = 1.73 Å, and Mo—O(3′) = 2.25 Å.[10]

conductivity, good photocatalytic activity, and remarkable electrochemical energy storage performance.[22–24] In this work, we presented a new method for the preparation of $Ag_2Mo_2O_7$ and Ag_2MoO_4 by reacting with Ag NPs, MoS_2, and oxygen gas in the air was investigated.

Experimental

Materials. Analytically pure MoS_2 (< 2 μm, 99%, Sigma-Aldrich, St. Louis, MO), LiF (~325 Mesh, 98.5%, Alfa Aesar, Lancashire, UK), $AgNO_3$ (ACS reagent, ≥ 99.8%, Sigma-Aldrich), and $NaBH_4$ (Sigma-Aldrich) were used as received. Water was distilled and further purified using a Millipore MilliQ system.

Sample Preparation

Preparation of α-MoO_3 by the Thermal Reaction of MoS_2 in Air. MoS_2 (1 g) was ground in a mortar and transferred to an alumina crucible. The sample was heated at 400°C for 4 h in an electric furnace and the rate at which the temperature increases was 5^0/min. This process was repeated at 500, 600, 700, 800, and 900°C.

Preparation of Li_2MoO_4 by the Thermal Reaction of MoS_2 with LiF (MoS_2:LiF = 1:5) in Air. MoS_2 (2.24 g, 14.0 mmol) and LiF (1.77 g, 68.2 mmol) were ground in a mortar and transferred to an alumina crucible. The sample was heated at 400°C for 4 h in an electric furnace. This process was repeated at 500, 600, 700, 800, and 900°C.

Preparation of MoO_2 by the Thermal Reaction of MoS_2 with LiF (MoS_2:LiF = 1:2) in Air. MoS_2 (2.00 g, 12.5 mmol) and LiF (0.648 g, 25.0 mmol) were ground in a mortar and transferred to an alumina crucible. The sample was heated at 400°C for 4 h in an electric furnace. This process was repeated at 500, 600, 700, 800, and 900°C. Sticky materials were observed over 600°C, and distilled water was used to recover the reaction products from the alumina crucible. The reaction products were filtered and the filtrate was transparent.

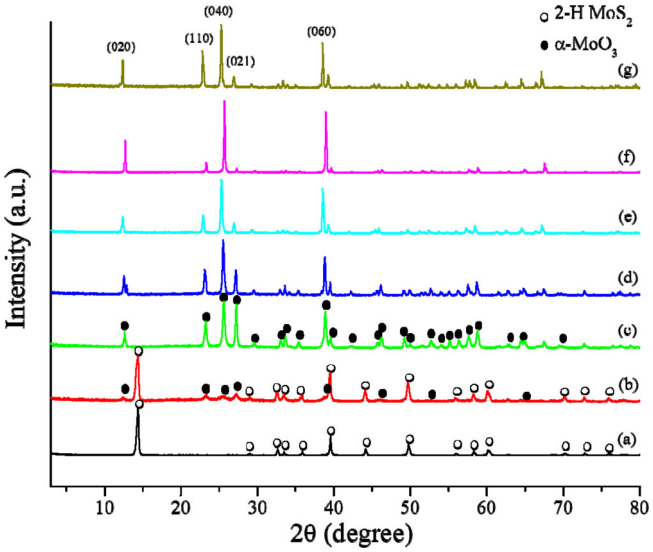

Figure 2. X-ray diffraction patterns of (a) commercial MoS_2 powder and MoS_2 powder heated in air at different temperatures: (b) 400°C, (c) 500°C, (d) 600°C, (e) 700°C, (f) 800°C, and (g) 900°C.

Preparation of Silver Molybdates by the Thermal Reaction of MoS_2 in the Presence of Silver Particles. MoS_2 (0.800 g, 5.00 mmol) and $NaBH_4$ (0.950 g, 25.0 mmol) in 500 mL of distilled water were vigorously stirred for 1 min. $AgNO_3$ (0.850 g, 5.00 mmol) in 200 mL of distilled water was prepared and silver colloids were gradually generated by slowly dripping the silver nitrate solution into the aqueous MoS_2 and $NaBH_4$ mixture. The slurry was stirred for 2 h, filtered, and thoroughly washed with distilled water. The sample was heated at 400, 500, 600, 700, 800, and 900°C for 4 h in an electric furnace.

Characterization. The prepared samples were analyzed by X-ray powder diffraction (XRD, PANalytical, X'Pert-PRO MPD, Almeldo, The Netherlands) using Cu Kα radiation (λ = 0.1540 nm). Powder morphologies were characterized using a Zeiss Supra 40 field emission scanning electron microscope (FESEM, SUPRA® 40 FE-SEM, Oberkochen, Germany) using an in-lens secondary electron detector.

Results and Discussion

Preparation and Characterization of α-MoO_3 Prepared by the Thermal Reaction of MoS_2 in Air. XRD was employed to characterize the crystalline structure and crystallinity of the as-made MoS_2 samples (Figure 2). The crystalline structure of the MoS_2 precursor was laminar with a weak interaction between the layers.[25,26] MoS_2 oxidized completely to α-MoO_3 at 500°C (Figure 2); however, it is stable at 500 and 700°C under vacuum (Figure 3).[27] This suggests that oxygen in the air was responsible for oxidizing MoS_2 to MoO_3 in this reaction. From Figure 2, the

conversion from MoS_2 to MoO_3 seems to proceed by MoS_2 completely decomposing rather than the stable MoS_xO_y structure forming. No peaks other than those of MoS_2 and α-MoO_3 were observed. Morphological changes of α-MoO_3 in air from 500 to 900°C were also investigated by XRD; although, at approximately 700°C α-MoO_3 began to sublime. The diffraction peaks at 500°C were assigned to orthorhombic α-MoO_3 (JCPDS card No. 05-0508), and no noticeable impurity peaks were observed. The strong diffraction peaks of the (020), (040), and (060) planes at 800°C showed highly anisotropic growth of the oxides with a layered crystal structure. The morphology of the α-MoO_3 samples was also characterized by SEM (Figure 4), and the observed morphological changes were consistent with those identified by XRD (Figure 2). The samples consisted entirely of stacked nanobelts corresponding to a high aspect (Figure 4(b) and (c)). The planar growth rates along the axes of the α-MoO_3 crystal are in the order of [001] > [100] > [010]; therefore, it is highly favorable for the growth of α-MoO_3 crystals along the [001] direction to give belt-like structures with the largest exposed surface being that of the (010) facets.[17,28] The main factor involved in the growth of α-MoO_3 belts is the reaction temperature. In this process, 800°C appeared to be the optimum temperature for the growth of α-MoO_3 belts. SEM examination showed that at 900°C, the length of α-MoO_3 along the [100] direction began to be expand due to sufficient energy for growth in this direction (Figure 4(d)). This result is consistent with that of the XRD experiment.

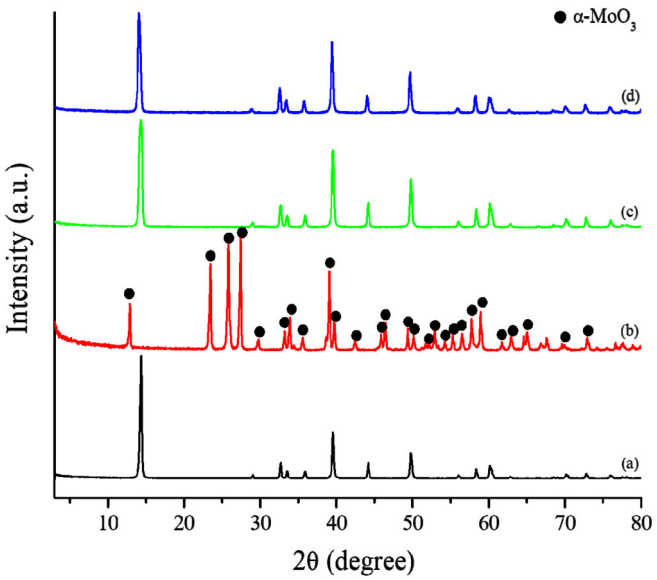

Figure 3. X-ray diffraction patterns of (a) commercial MoS_2 powder, (b) MoS_2 powder heated in air at 500°C and MoS_2/$Tb(NO_3)_3$ powder heated in vacuum at (c) 500°C, and (d) 700°C.

Preparation and Characterization of Molybdenum Oxides Prepared by the Thermal Reaction of MoS_2 with LiF in Air. MoO_3 has attracted significant attention as a key material in the field of lithium-ion batteries because of its high stability, which could accommodate the structural

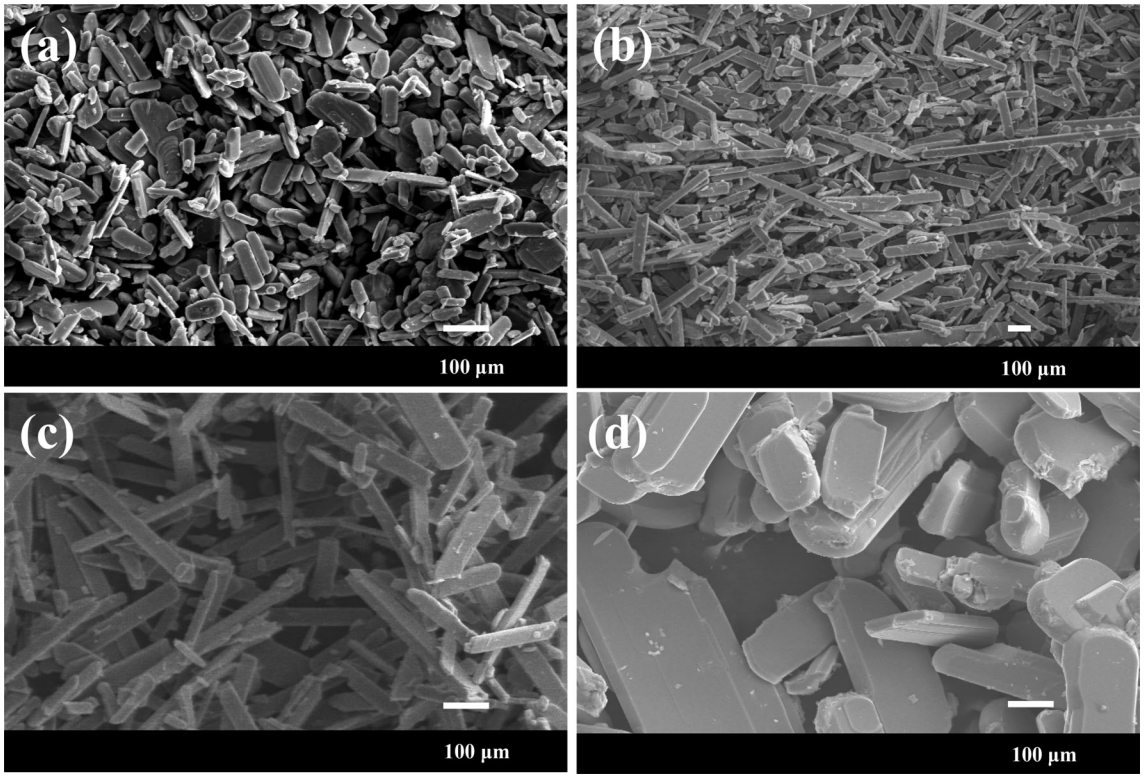

Figure 4. SEM micrographs of MoS_2 powder heated in air at different temperatures: (a) 600°C, (b) 700°C (c) 800°C, and (d) 900°C.

strain introduced by Li^+ insertion/extraction.[29] To obtain lithiated MoO_3, the thermal reaction of MoS_2 with LiF in air was employed.

Thermal Reactions of MoS_2 with LiF (MoS_2:LiF = 1:5) in Air. The XRD patterns of thermally treated MoS_2–LiF powders were observed at various temperatures (Figure 5). The formation of α-MoO_3 was observed at 400°C and nearly completed at 500°C. New phases over 600°C were identified until 900°C, with the major phase being Li_2MoO_4. The XRD patterns of the major phase (Figure 5) match those of Li_2MoO_4 (JCPDS Card No. 12-0763). Relatedly, a rhombohedral structure of Li_2MoO_4 was reportedly formed through the crystallization of slowly cooled LiF-MoO_3 fluxes in platinum crucibles in air.[30] The reaction product morphologies in the present study were analyzed using SEM, where stacked nanoplates with a width of ~4.4 μm and a length of ~56 μm were observed at 400°C (Figure 6(a)). These are stacked nanoplates of α-MoO_3. These stacked nanoplates prevailed at 500°C, but at temperatures greater than 600°C, the morphology of the reaction products completely changed. These observations are consistent with those of the XRD experiments (Figure 5). Other minor phases that were detected are unknown, and further purification is needed.

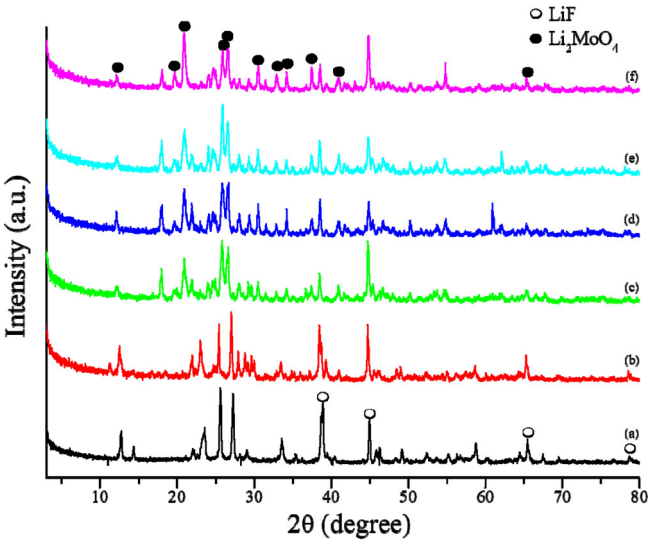

Figure 5. X-ray diffraction patterns of MoS_2/LiF (MoS_2:LiF = 1:5) powder heated in air at different temperatures: (a) 400°C, (b) 500°C, (c) 600°C, (d) 700°C, (e) 800°C, and (f) 900°C.

Thermal Reactions of MoS_2 with LiF (MoS_2:LiF = 1:2) in Air. To obtain pure Li_2MoO_4, the stoichiometry of the Li^+ ions was adjusted with MoS_2 to give Li_2MoO_4. Li_2MoO_4 is highly hygroscopic; thus, distilled water was used to recover the reaction products obtained over 600°C from the alumina crucible. The reaction products were filtered and dried in air. Because the amount of dried sample was large, the sample was analyzed by XRD. The XRD patterns of thermally treated MoS_2/LiF (MoS_2:LiF = 1:2) powders at various temperatures were collected, where the formation of α-MoO_3 was observed at 400°C and nearly completed at 500°C (Figure 7). Furthermore, dried samples over 600°C were matched to crystalline monoclinic MoO_2 (JCPDS Card No. 32-0671). No impurity peaks were observed. Generally,

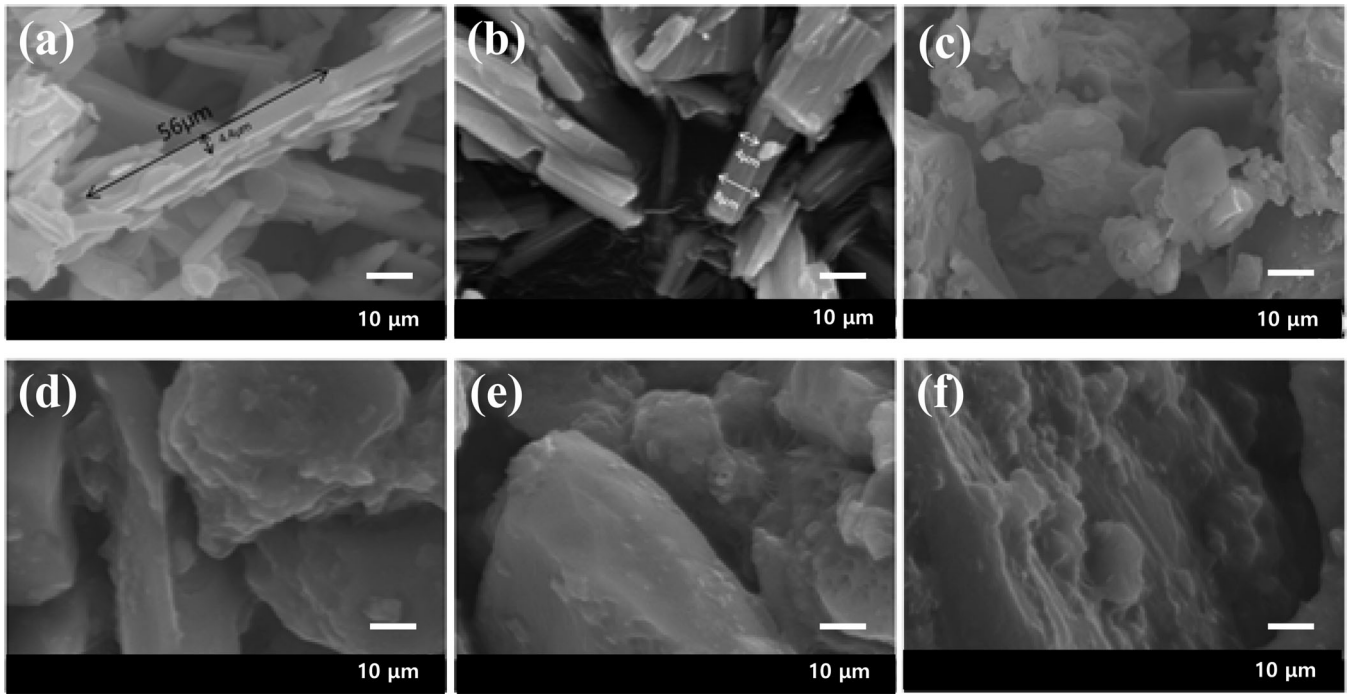

Figure 6. SEM micrographs of MoS_2/LiF (MoS_2:LiF = 1:5) powder heated in air at different temperatures: (a) 400°C, (b) 500°C, (c) 600°C, (d) 700°C, (e) 800°C, and (f) 900°C.

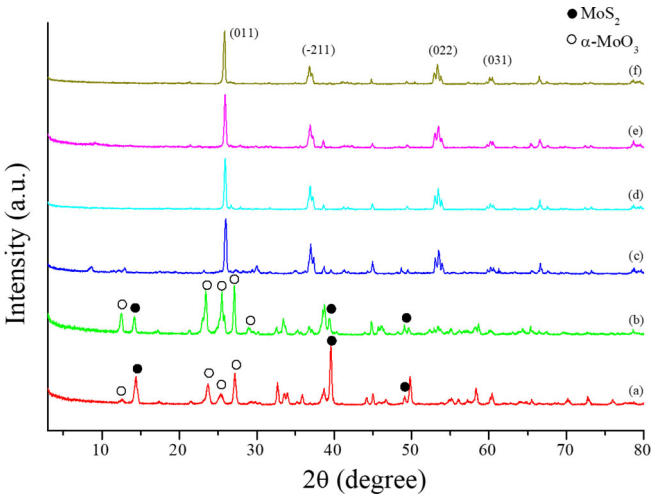

Figure 7. X-ray diffraction patterns of MoS_2/LiF (MoS_2:LiF = 1:2) powder heated in air at different temperatures: (a) 400°C, (b) 500°C, (c) 600°C, (d) 700°C, (e) 800°C, and (f) 900°C.

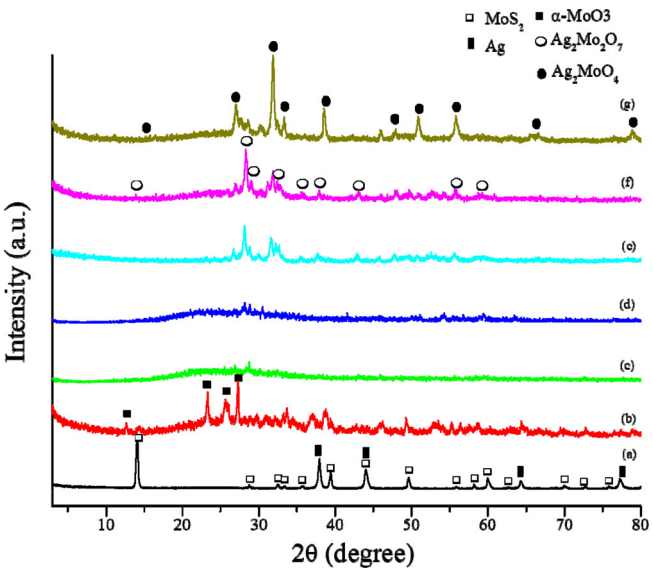

Figure 8. X-ray diffraction patterns of MoS_2/Ag powder heated in air at different temperatures: (a) room temperature, (b) 400°C, (c) 500°C, (d) 600°C, (e) 700°C, (f) 800°C, and (g) 900°C.

MoO_2 is prepared by reducing MoO_3 under a hydrogen atmosphere at approximately 800°C. On the other hand, we obtained MoO_2 by reacting MoS_2 with LiF (MoS_2:LiF = 1:2) at the relatively low temperature of 600°C.

Preparation and Characterization of $Ag_2Mo_2O_7$ and Ag_2MoO_4 Prepared by the Thermal Reaction of MoS_2 with ag Nanoparticles in Air. Molybdenum disulfide (MoS_2) has a lamellar structure in which the atoms within a plane are held together by covalent bonds, which are stronger than the van der Waals interactions between the planes. This allows the basal planes to easily slide over one another. Thus, MoS_2 is widely used in industry as a solid lubricant with excellent friction and wear properties. However, its application in humid environments and at high temperatures is limited due to reactions with water and oxygen.[31] To solve these problems, a recent study[32] showed that integrating Ag nanoparticles (NPs) into MoS_2 improved tribological performance, especially in high-temperature applications. In this study, products from the thermal reactions of MoS_2-Ag NPs at various temperatures in air were monitored by XRD to identify the main components formed in this process.

MoS_2 and Ag NPs were heated at 400–900°C for 4 h in an electric furnace and the XRD patterns of the prepared samples were collected at different temperatures (Figure 8) using the solid-state reaction method. At 400°C, most of the MoS_2 had converted to MoO_3 and the Ag NPs became smaller, where peak broadening of the silver particles was evident. Amorphous phases were observed at 500–600°C, and a new phase of $Ag_2Mo_2O_7$ was observed at 700°C. All the diffraction peaks at 700°C were indexed to the cubic phase of $Ag_2Mo_2O_7$ (JCPDS Card No. 75-1505). No characteristic peaks belonging to other impurities were detected, indicating that the synthesis provided pure product. At 900°C, new major peaks appeared and were indexed as the cubic phase of Ag_2MoO_4 (JCPDS Card No. 75-250). This reaction can be described as follows:

$$Ag_2Mo_2O_7 \rightarrow Ag_2MoO_4 + MoO_3 \rightarrow \text{Other products}$$

These results are similar to those observed when fabricating thin films of MoO_3-Ag_2O high-temperature lubricants. Three phases, $Ag_2Mo_2O_7$, Ag_2MoO_4, and $Ag_2Mo_4O_{13}$, have been identified in the deposited films. Among these, single-phase Ag_2MoO_4 thin films behave very well as a lubricant over the wide temperature range of 100–600°C.[33]

Conclusion

MoS_2 is thermally active and easily oxidized in air to give α-MoO_3. For these reasons, it is interesting to study whether MoS_2 can facilitate the generation of useful molybdenum oxides. MoS_2 easily loses sulfide and reacts with oxygen gas upon heating in air to give a variety of molybdenum oxides. In the presence of LiF, MoS_2 reacted with oxygen gas in the air to generate Li_2MoO_4 and MoO_2, depending on the concentration of LiF. In the presence of Ag NPs, MoS_2 reacted with oxygen gas in the air to generate $Ag_2Mo_2O_7$ and Ag_2MoO_4, depending on the heating temperature. These results demonstrate that MoS_2 is an important precursor for generating useful molybdenum oxides on the surface of inert substrates without requiring sophisticated equipment. Furthermore, these oxides could likely exhibit morphological versatility by introducing appropriate ligands and changing experimental conditions.

Acknowledgments. The present research was supported by the research fund of Dankook University in 2019.

References

1. J. Scholz, A. Walter, A. H. P. Hahn, T. Ressler, *Micropor. Mesopor. Mater* **2013**, *180*, 130.
2. T. Leisegang, D. C. Meyer, A. A. Levin, S. Braun, P. Paufler, *Appl. Phys. A* **2003**, *77*, 965.
3. J. R. C. Rocha, L. Kosminsky, T. R. L. C. Paixao, M. Bertotti, *Electroanalysis* **2001**, *13*, 155.
4. K. Galatsis, Y. X. Li, W. Wlodarski, E. Comini, G. Sberveglieri, C. Cantalini, S. Santucci, M. Passacantando, *Sens. Actuators B* **2002**, *83*, 276.
5. J. N. Yao, K. Hashimoto, A. Fujishima, *Nature* **1992**, *355*, 624.
6. C. Bechinger, S. Ferrere, A. Zaban, J. Sprague, B. A. Gregg, *Nature* **1996**, *383*, 608.
7. C. G. Granqvist, *Sol. Energy Mater. Sol. Cells* **2008**, *92*, 203.
8. J. Y. Hwang, K. M. Ok, *Bull. Kor. Chem. Soc.* **2020**, *41*, 588.
9. Y. S. Jeong, Y. J. Jang, S. J. Park, Y. J. Lee, *Bull. Kor. Chem. Soc.* **2019**, *40*, 642.
10. Z. Y. Hsu, H. C. Zeng, *J. Phys. Chem. B* **2000**, *104*, 11891.
11. W. Cho, J. H. Song, J. H. Kim, G. Jeong, E. Y. Lee, Y. J. Kim, *J. Appl. Electrochem.* **2012**, *42*, 909.
12. Z. Wang, S. Madhavi, X. W. Lou, *J. Phys. Chem. C* **2012**, *116*, 12508.
13. S. Hu, X. Ling, T. Lan, X. Wang, *Chem. Eur. J.* **2010**, *16*, 1889.
14. K. Shao, H. Kuo, H. Cao, *J. Mater. Res.* **2008**, *23*, 2602.
15. X. L. Li, J. F. Liu, Y. D. Li, *Appl. Phys. Lett.* **2002**, *81*, 4832.
16. V. Lavayen, N. Mirabal, J. Seekamp, C. M. S. Torres, E. Benavente, G. González, *Phys. Stat. Sol. C* **2004**, *1*, S58.
17. L. Cheng, M. Shao, X. Wang, H. Hu, *Chem. Eur. J.* **2009**, *15*, 2310.
18. Q. Li, S. Fan, W. Han, C. Sun, W. Liang, *Jpn. J. Appl. Phys. (Part 2)* **1997**, *36*, L501.
19. F. Jin, Y. Liu, C. M. Day, S. A. Little, *Carbon* **2007**, *45*, 587.
20. W. Shen, H. Wang, R. Guan, Z. Li, *Colloids Surf. A* **2008**, *331*, 263.
21. M. Salavati-Niasari, S. N. Mirsattari, M. Bazarganipour, *Polyhedron* **2008**, *27*, 3653.
22. W. M. R. Divigalpitiya, R. F. Friendt, S. R. Morrison, *Science* **1989**, *246*, 369.
23. J. V. Kumar, R. Karthik, S. M. Chen, V. Muthuraj, C. Karuppia, *Sci. Rep.* **2016**, *6*, 34149.
24. S. Bhattacharya, A. Ghosh, *Phys. Rev. B* **2007**, *75*, 092103.
25. A. K. Arora, R. Nithya, S. Misra, T. Yagi, *J. Solid State Chem.* **2012**, *196*, 391.
26. G. Eda, H. Yamaguchi, D. Voiry, T. Fujita, M. Chen, M. Chhowalla, *Nano Lett.* **2011**, *11*, 5111.
27. Initially, this experiment was designed to make MoS_2/Tb Phosphors. Very small amount of $Tb(NO_3)_3$ was used.
28. X. W. Lou, H. C. Zeng, *Chem. Mater.* **2002**, *14*, 4781.
29. L. Mai, B. Hu, W. Chen, Y. Qi, C. Lao, R. Yang, Y. Dai, Z. L. Wang, *Adv. Mater.* **2007**, *19*, 3712.
30. U. Kolitsch, *Z. Kristallogr* **2001**, *216*, 449.
31. A. Erdemir, *Surf. Coat. Technol.* **2005**, *200*, 1792.
32. W. Zhang, D. Demydov, M. P. Jahan, K. Mistry, A. Erdemir, A. P. Malshe, *Wear* **2012**, *288*, 9.
33. W. Gulbiński, T. Suszko, *Wear* **2006**, *261*, 867.

